Hindawi
International Journal of Chemical Engineering
Volume 2024, Article ID 6346033, 14 pages
https://doi.org/10.1155/2024/6346033

Research Article

Investigating the Adsorption of Humic Acid from Water Using CTS/PAM and CTS/PAM/EDTA Adsorbents

Mahdi Alizadeh,[1] Sajjad Abdi,[1] S. Majid Abdoli ,[1] Hossein Hazrati ,[1] and Mehdi Salami-Kalajahi [2]

[1]*Faculty of Chemical Engineering, Sahand University of Technology, P.O. Box 51335-1996, Sahand, Tabriz, Iran*
[2]*Faculty of Polymer Engineering, Sahand University of Technology, P.O. Box 51335-1996, Sahand, Tabriz, Iran*

Correspondence should be addressed to S. Majid Abdoli; abdoli@sut.ac.ir and Hossein Hazrati; h.hazrati@sut.ac.ir

Received 24 October 2023; Revised 17 March 2024; Accepted 9 April 2024; Published 24 April 2024

Academic Editor: Voon-Loong Wong

In recent decades, reports from around the globe indicate an increase in natural organic matters (NOMs) in surface waters, which has a negative impact on drinking water purification and causes problems such as the taste and color of water, reducing the amount of dissolved oxygen in water, causing membrane fouling in the filtration process, and acting as a precursor for the formation of an antiseptic by-product. This work used the adsorption process to evaluate the elimination of natural organic compounds in aquatic environments. Ethylenediaminetetraacetic acid (EDTA) as a crosslinker for chitosan (CTS) and N, N-methylenebisacrylamide as a crosslinker for polyacrylamide (PAM) were used to prepare humic acid (HA) adsorbents utilizing a two-step procedure. The FTIR spectroscopy proved the EDTA cross-linking agent was effective with the semicrosslinking CTS/PAM hydrogel. CTS/PAM/EDTA double network (DN) hydrogel exhibited a higher HA adsorption capacity (q_e = 107.7 mg/g) than CTS/PAM (q_e = 59.3 mg/g) at pH = 7 and an initial concentration of 60 mg·L^{-1} during 60 min. Also, results demonstrate that CTS/PAM/EDTA DN hydrogels showed faster adsorption kinetics than CTS/PAM.

1. Introduction

Natural organic materials (NOMs) are the most abundant component in the aquatic environment [1, 2]. They may be found in all freshwater, particularly surface water, due to interactions between the hydrological cycle, the biosphere, and the geosphere. Natural organic matter is defined as a complex mixture of heterogeneous organic molecules such as humic substances, polysaccharides, amino acids, proteins, peptides, lipids, and hydrophilic acids [3, 4]. Humic acid (HA) constitutes the major fraction of NOMs practically present in all drinking water sources [5]. The substance is obtained from the decomposition of organic matter from plants and animals found in both water and land habitats [6]. They vary significantly in chemical composition, molecular size, molecular weight (humic substances have molecular weights ranging from a few hundred to ten thousand), and structure [7]. The presence of humic acid in drinking water sources leads to several issues in water treatment and distribution systems. Humic acid negatively impacts water quality by generating undesirable odors, flavors, and discoloration in drinking water [8]. It also creates metal complexes that are more difficult to treat, encourages the growth of bacteria in water distribution systems, and reacts with chlorine to produce carcinogenic disinfection by-products (DBPs) that are harmful to human health [9, 10]. Various human health concerns, among others, necessitate the removal of humic acid from water, making it a crucial step at water treatment plants [11]. Regrettably, the standard water treatment procedure, which includes coagulation, flocculation, sedimentation, and filtering, can only eliminate 10–50% of the humic acid [12].

NOMs are complex mixes of distinct molecules with diverse functional groups, such as ester, phenol, quinine, carboxylic, hydroxyl, and amine, all with a negative charge at neutral pH [13]. Humic compounds give water a yellowish to

a brownish hue. Additionally, ground and surface water are contaminated due to the humic compounds' high propensity for complexation with contaminants such as heavy metals and pesticides [14]. In addition, during the chlorination step of water, HA will form very toxic DBPs, i.e., chlorinated organic compounds such as trihalomethanes (THMs) that exhibit mutagenic properties [15, 16]. The molecular structure of HA is available in Figure S1 (in the supporting information). The World Health Organization (WHO) has stated that the guideline values for DBPs in drinking water should not exceed 100 μg/L which makes the HA removal process from water more crucial [17]. Furthermore, HA is one of the causes of fouling in the membrane bioreactor [18]. Effective HA removal techniques include adsorption [19, 20], activated carbon [21, 22], clays [23, 24], zeolite [25], chitosan [26], metal-modified silica [26], and mesoporous silica [27] are only a few of the adsorbents that have been used for HA adsorption throughout the years [28].

Hydrogel, a type of polymeric substance, is characterized by its insoluble swelling and the capacity to hold a large amount of water inside its structure [29]. A hydrogel's polymer chain has a lot of hydrophilic functional groups, including carboxyl, hydroxyl, and amino [29–31]. The mechanical characteristics of many natural polymer hydrogels, including polysaccharides and proteins, are subpar [30]. While the mechanical capabilities of synthetic polymer hydrogels surpass those of natural polymer hydrogels, most networks created by chemical crosslinking techniques are brittle and irreparably shattered when subjected to severe strain [32]. The result is that hydrogels have negligible mechanical strength [30].

Gong et al. [33] first introduced the concept of DN hydrogels in 2003 using a two-step, sequential free-radical polymerization method. They proposed that the unique entangled network topology of their hydrogel would significantly enhance its mechanical properties. The novel network structure consisted of two networks, one being stiff and strongly crosslinked and the other being ductile and loosely crosslinked. As a result of the nonlinear interactions between the two networks, this novel structure provided greater mechanical strength [34]. The hydrogel's mechanical properties were enhanced by introducing more irregularity into its DN structure. DN hydrogels are distinguished from typical gels due to their significant advancements in mechanical characteristics [35]. Historically, DN hydrogels have had poor self-healing characteristics because their two chemically crosslinked (covalent crosslinked) networks are robust but challenging to recover from injury [30].

The introduction of physically crosslinked DN hydrogels led to excellent anti-swelling performance [36, 37] and self-healing capabilities [38, 39], thanks to the presence of weak and reversible noncovalent bonds. It is possible to enhance the hydrogel's mechanical characteristics, anti-swelling performance, and self-healing abilities by including weak and reversible bonds rather than relying on chemically crosslinked ones [40, 41]. Additionally, the hydrogel can exhibit electrochemical capabilities, depending on the positive/negative charge of network groups like carboxyl and amino at a particular pH. DN hydrogels have garnered more attention because of their unique characteristics [42, 43].

The network architectures of DN hydrogels are often modified [44]. Due to extensive study, several systems of DN hydrogels have been produced, each with improved mechanical characteristics, easier production processes, cheaper raw ingredients, and a wider range of potential applications. Some hydrogels are employed as adsorbents to remove pollutants (dyes [45], heavy metals [46, 47], antibiotics [48, 49], etc.) from the environment. This is only one example of the many environmental uses of hydrogels that have emerged in recent years. Some DN hydrogels are employed as pesticide delivery systems, where the hydrogel chain diffuses and relaxes while the pesticide diffusion process takes place simultaneously [50]. This is conceivable because DN hydrogels charged functional groups can easily accept ions into their swollen structures.

This study evaluates the efficiency of CTS/PAM and CTS/PAM/EDTA on HA adsorption in aquatic media. The synthesized adsorbents are analyzed both kinetically and using different adsorption isotherms. Compared to pure CTS, CTS and PAM can form a composite with enhanced properties. PAM can improve CTS's mechanical stability and adsorption capacity, potentially leading to better performance in HA adsorption from water [51, 52]. Additionally, PAM is known for its high solubility in water, which can facilitate the dispersion of CTS/PAM in water and increase the contact between the adsorbent and the target pollutant [53]. It is worth mentioning that the effectiveness of CTS/PAM and CTS/PAM/EDTA in adsorbing HA is influenced by several factors, such as the concentration of the adsorbents, pH, temperature, contact time, initial HA concentration, and properties of the water being treated (such as water chemistry, presence of competing ions, and organic matter). Hence, it is imperative to conduct experimental research, encompassing kinetic and isotherm analyses, to ascertain the precise adsorption efficiency and performance of CTS/PAM and CTS/PAM/EDTA for removing HA from water under specified conditions.

2. Methods

2.1. Materials. Chitosan ($C_{56}H_{103}N_9O_{39}$, Sigma-Aldrich), acrylamide (C_3H_5NO, Sigma-Aldrich), N,N-methylene bisacrylamide ($C_7H_{10}N_2O_2$, Sigma-Aldrich), humic acid ($C_9H_9NO_6$, Sigma-Aldrich), ammonium persulfate ($(NH_4)_2S_2O_8$, Sigma-Aldrich), dimethyl sulfoxide (C_2H_6OS, Sigma-Aldrich), ethylenediaminetetraacetic acid (EDTA, $C_{10}H_{16}N_2O_8$, Sigma-Aldrich), pyridine (C_5H_5N, Merck), diethyl ether ($(C_2H_5)_2O$, Merck), and acetic anhydride ($C_4H_6O_3$, Sigma-Aldrich) were used in this research for CTS/PAM and CTS/PAM/EDTA hydrogels synthesis.

2.2. Preparation of EDTA Dianhydride. A 100 mL flask with a condenser and a magnetic stirrer was filled with 20 g of EDTA, 16 mL of pyridine, and 28 mL of acetic anhydride. The reaction was conducted at 65°C for 24 h. Acetic

anhydride and diethyl ether were used to filter and thoroughly wash the EDTA dihydride. The white cream was then ground into a white powder and dried for 24 h at 65°C in a vacuum oven [54]. Figure S2 (in the supporting information) represents the synthesis of EDTA dianhydride.

2.3. Characterization. The Microtrac-Nanotrac Wave equipment was utilized to perform zeta potential analysis in order to investigate the surface charge of the generated adsorbents at different pH levels. To prepare the samples for the test, we dissolved 0.001 g of each sample in 10 ml of distilled water and then exposed them to ultrasonic treatment for 5 minutes.

The field emission scanning electron microscopy (FE-SEM, MIRA3 TESCAN) was used to evaluate the morphology and surface structure of the materials. Fourier-transform infrared spectroscopy (FTIR, TERMO AVATAR) was employed to investigate the functional groups of the materials. The HA concentration in the aqueous solution was measured using UV spectroscopy while the adsorption process was taking place.

2.4. Preparation of CST/PAM Hydrogel. Initially, solution A was prepared by stirring 3 g chitosan in 72 mL of 1 *vol.* % acetic acid solution in a 100 mL flask at 60°C for 1 h. Then, 12 mL of deionized water was mixed with 6 g of acrylamide, and 1 mol. % methylenebisacrylamide as a crosslinker was added to prepare solution B. In the next step, a 0.3% solution of ammonium persulfate as an initiator (2 mL) was added to solution A, which was agitated for 10 min at 60°C. Afterward, solution A was cooled to room temperature. Solutions A and B were mixed at room temperature to provide a homogenous solution. Finally, the solution was injected into a 50-mL beaker and heated in an oven at 60°C for 6 h. The resulting gel was washed several times with methanol and soaked for 24 h in a methanol solution to eliminate contaminants and unreacted compounds. The gel was then oven-dried for 6 h at 60°C. Figure 1 depicts the molecular structure of the CTS/PAM network.

2.5. Preparation of CST/PAM/EDTA Hydrogel. To synthesize the CST/PAM/EDTA DN hydrogel, the resulting gel was submerged in 120 mL of dimethyl sulfoxide containing EDTA dianhydride for 12 h at 60°C. After obtaining the gel, it was washed several times with methanol and then soaked in a methanol solution for 24 h to eliminate any remaining contaminants or unreacted materials. The product was then dried in an oven at 60°C for 6 h. Figure 2 represents the molecular structure of the CTS/PAM/EDTA DN hydrogel.

2.6. Adsorption Process Methodology. The pH of the solution was brought up to 10 using NaOH, and the mixture was agitated for 24 to prepare the HA solution in various concentrations. Finally, HCl was used to decrease the pH to 7. At 4°C, the produced solution was stored in the darkness a. Afterwards, the HA solution of 60 mg/L and adsorbent amount of 25 mg was investigated at room temperature and neutral pH. After each test, HA is analyzed using a UV spectrophotometer and a quartz cell with a 254 nm length was used to create its calibration curve. The final concentrations were calculated following the intended trials using the device's specified absorption number and in accordance with the calibration curve. After each test, the transfer solution is sufficiently run through the paper for the final determination. The filtered solution is then poured into the quartz cell, and after adjusting the apparatus, the desired absorbance is read at a wavelength of 254 nm. It was possible to convert the absorbance value displayed by the combined calibration curve of the solution (C) in each experiment. HA adsorption calibration diagram is depicted in Figure 3. The adsorption capacity was calculated using equation [55]:

$$q_e = (C_0 - C_e)\frac{V}{m}, \tag{1}$$

where C_0 and C_e represent the initial and equilibrium concentrations of the adsorbate in solution (mg/L), respectively, while q_e denotes the adsorption capacity (mg/g) of the adsorbent at equilibrium. V and m signify the volume of solution (L), and the mass of the adsorbent (g), respectively.

In addition, the amount of adsorption at different times was calculated using equation (2) [55]:

$$q_t = (C_0 - C_t)\frac{V}{m}, \tag{2}$$

where q_t and C_t are the amount of adsorption (mg/g) and concentration(mg/L), respectively, at time t (mg/g).

Nonlinear regression was conducted utilizing SigmaPlot 12 software [56], incorporating relevant isotherm equations within its equation category. This selection was made based on the software's capability to promptly generate statistical error analysis outcomes, such as the coefficient of determination (R^2), along with the regression results for isotherm and kinetic parameters [57]. The utilization of this statistical data enables a comprehensive understanding of the inherent limitations present in each equation. Furthermore, regression analysis was employed to fit different adsorption isotherms with experimental adsorption data and also pseudo-first-order, pseudo-second-order, and intraparticle diffusion kinetic models to the experimental kinetic data.

3. Results and Discussion

3.1. FTIR of CTS/PAM and CTS/PAM/EDTA. In all three spectra, as shown in Figure 4, there is a reasonably strong peak in the vicinity of wavenumbers of 3200–3500 cm^{-1} (points a), which is connected to the carbohydrate ring's O-H stretching bond and the overlap of the N-H stretching vibration. The saccharide ring (wavenumbers of 1030, 1116, and 1160 cm^{-1}), first-type amide vibrations (1650), and second-type amide (1591) are responsible for the majority of the peaks in chitosan [58]. A brand-new peak in the CTS/PAM hydrogel appeared in the 3180–3185 range (point b), which denotes the stretching vibration of the amine group–NH. In the region between 1650 and 1640 (point c),

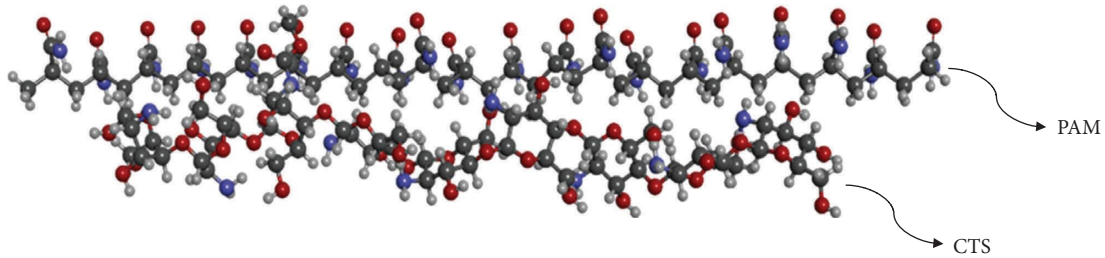

Figure 1: Schematic representation of CTS/PAM network.

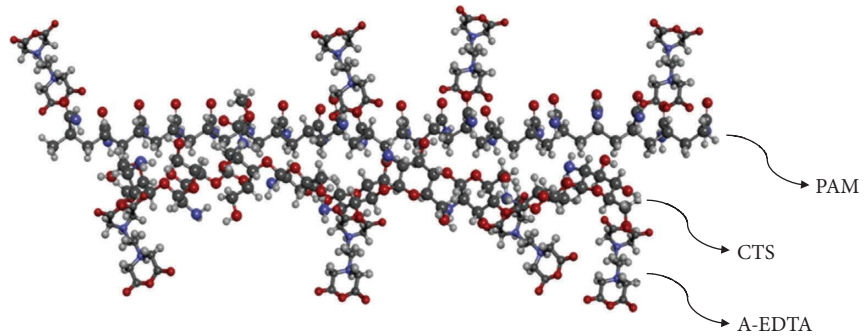

Figure 2: Schematic representation of CTS/PAM/EDTA DN hydrogel.

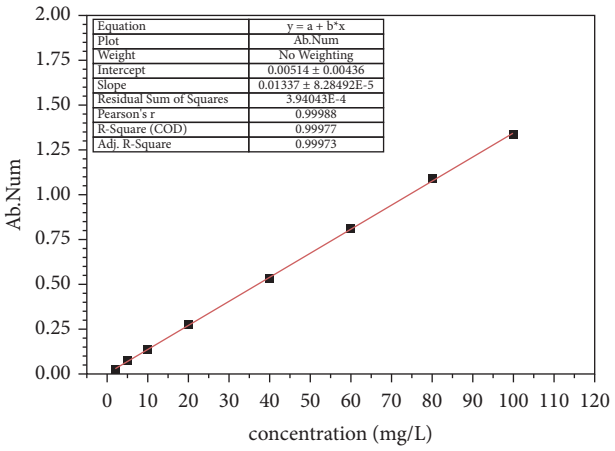

Figure 3: HA adsorption calibration diagram.

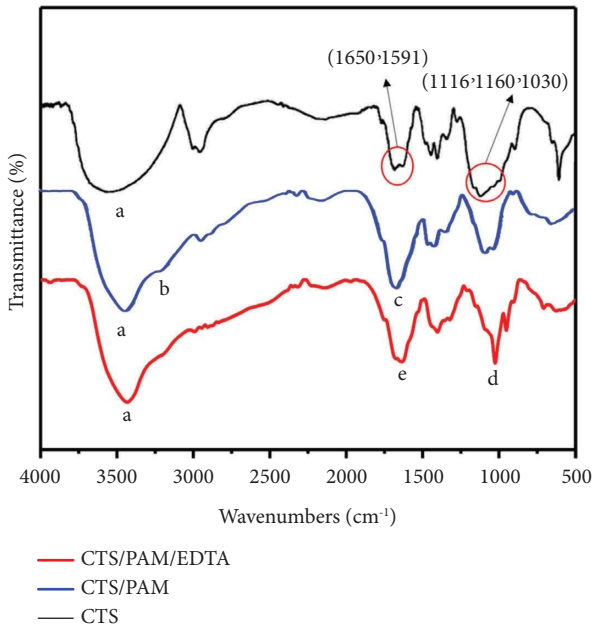

Figure 4: FTIR spectra of CTS/PAM and CTS/PAM/EDTA hydrogels.

the vibration of the first- and second-type amine groups overlaps with a bond and is connected to the stretching vibration of the C=O group [59]. The peak of the saccharide ring coincides with a distinct band at 1115 (point d) in the CTS/PAM/EDTA DN hydrogel, which is connected to the stretching vibration of the carboxylic group. The peak between 1590 and 1600 (vibration bond N-H) indicates that the EDTA dianhydride and NH_2 groups were successfully crosslinked (point e).

3.2. SEM Images of CTS/PAM and CTS/PAM/EDTA Hydrogels. Figures 5(a) and 5(b) shows the SEM images of the CTS/PAM hydrogel structure. As shown, the hydrogel has an interwoven porous network. The lines indicate transverse connections, which are characteristics of the hydrogel morphology. The porosity of the CTS/PAM hydrogel is heterogeneous due to the semi-crosslinked polymer network. The SEM images of CTS/PAM/EDTA DN hydrogel are illustrated in Figures 5(c) and 5(d). As shown, the surface roughness has reduced, indicating that the EDTA synthesis on CTS/PAM was effective. The subsequent cross-linking induced by EDTA drastically decreases the pore size of the hydrogel network.

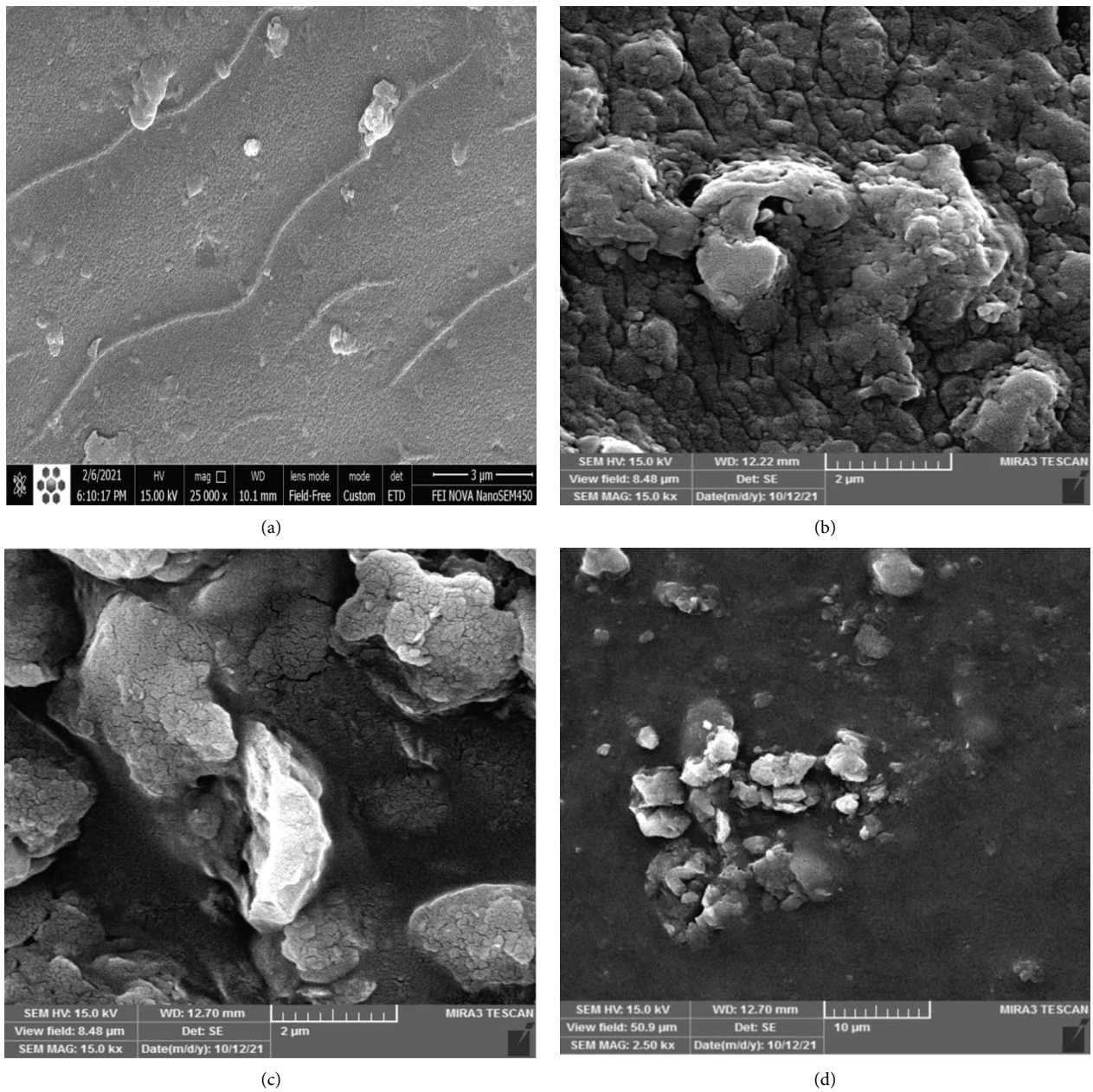

Figure 5: SEM images of (a) and (b) CTS/PAM hydrogel, and (c) and (d) CTS/PAM/EDTA hydrogel.

3.3. The Adsorption Kinetics. The findings of adsorption tests on CTS/PAM semi-cross network hydrogel adsorbents and CTS/PAM/EDTA hydrogel with DN agent are shown in Table 1.

According to the findings of the adsorption kinetics for the CTS/PAM semi-mutual network hydrogel, as shown in Figure 6, the adsorption of HA increased over time and followed an upward trend. Based on these data, the propensity to adsorb as much HA as possible from an aqueous environment rises dramatically during the first 90 min but does not vary much afterward. In addition, the increasing trend of HA adsorption by CTS/PAM/EDTA DN hydrogel has persisted for an extended duration of 60 min, as can be seen in Figure 6. Therefore, the adsorption process trends toward a nearly constant value after this time. Comparing the performance and rate of adsorption of the two adsorbents reveals that the CTS/PAM/EDTA DN hydrogel has a greater adsorption rate under identical circumstances. This is due to the existence of more active adsorption sites in the DN hydrogel structure [60]. As the adsorption process proceeds, the active sites become progressively occupied, and the adsorption rate reduces owing to the repulsive interactions between the HA molecules in the aqueous solution and the molecules on the adsorbent surface [61]. Finally, when there was no adsorption, a balance was attained. Figure 6 depicts the time-dependent adsorption

Table 1: Kinetic model parameters for HA adsorption process for both adsorbents.

Kinetic models	Parameters	CTS/PAM	CTS/PAM/EDTA
Pseudo-first-order	k_1(g·mg^{-1}·min^{-1})	0.0132	0.0367
	$q_{e,cal}$ (mg·g^{-1})	118.64	111.63
	R^2	0.942	0.971
	$q_{e,exp}$	106.14	104.54
Pseudo-second-order	k_2(g·mg^{-1}·min^{-1})	7.56×10^{-5}	3.43×10^{-4}
	$q_{e,cal}$ (mg·g^{-1})	154.01	127.29
	R^2	0.918	0.939
	$q_{e,exp}$	106.14	104.54
Intraparticle diffusion	k_i(g·mg^{-1}·min$^{-1/2}$)	8.76	19.42
	R^2	0.912	0.954
	$q_{e,cal}$(mg·g^{-1})	66.21	120.41
	C (mg·g^{-1})	−16.89	−30.02

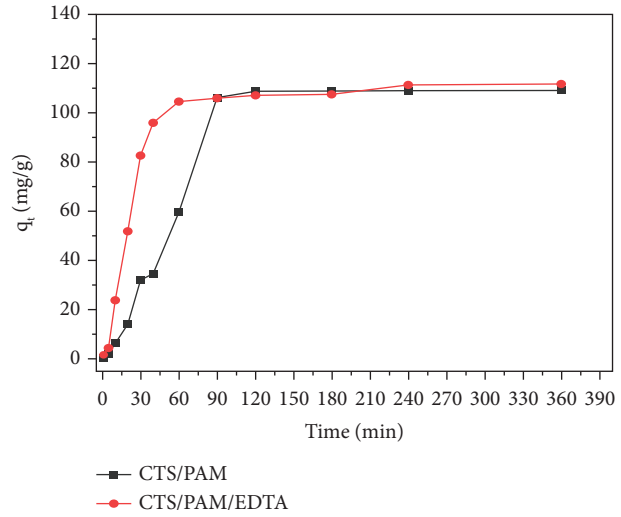

Figure 6: Adsorption kinetics for CTS/PAM and CTS/PAM/EDTA hydrogels.

capacities of CTS/PAM semi-cross network hydrogel adsorbents and CTS/EDTA DN hydrogel. Detailed information can be found in Section 2 of the supporting information.

Pseudo-first-order and pseudo-second-order kinetic models, as well as the intraparticle diffusion model, were utilized to evaluate the adsorption rate and potential adsorption mechanism during HA removal using chosen adsorbents. The rate-limiting mechanism of the process is thought to be physical adsorption in the pseudo-first-order kinetic model [55, 62]. On the other hand, in the pseudo-second-order kinetic model [63], chemical adsorption is regarded as the rate-limiting mechanism of the adsorption process.

The best kinetic model for CTS/PAM can be developed by comparing the findings shown in Table 1 and may be described as a pseudo–first-order kinetic model with $R^2 = 0.942$ and $q_{e,cal} = 118.64\ mg{\cdot}g^{-1}$. The pseudo–first–order kinetic model for the CTS/PAM/EDTA adsorbent produced $R^2 = 0.971$ and $q_{e,cal} = 111.63\ mg{\cdot}g^{-1}$, indicating that it is the best kinetic model that has been offered for this adsorbent. The findings for both adsorbents indicate that physical adsorption is the regulating step, and electrostatic and hydrophilic interactions are the adsorption mechanisms [64, 65].

The pseudo-first-order kinetic model for CTS/PAM and CTS/PAM/EDTA hydrogels is shown in Figure 7(a) with $R^2 = 0.942$ and $q_{e,cal} = 118.64\ mg{\cdot}g^{-1}$ for CTS/PAM and $R^2 = 0.971$ and $q_{e,cal} = 111.63\ mg{\cdot}g^{-1}$, respectively. It is evident that the data have a good match and a well-fitting curve. For CTS/PAM/EDTA, it is visible. The adsorption capacity value calculated using the pseudo-first-order model agreed with the results of the experiments.

As depicted in Figure 7(b), the results of fitting the sketched curves for the CTS/PAM and CTS/PAM/EDTA hydrogel absorbents revealed that the $q_{e,cal}$ values for the pseudo-second-order model of fitting with $R^2 = 0.918$ and $R^2 = 0.939$, respectively, were lower than those for the pseudo-first-order model. The adsorption capacity value predicted by the pseudo-second-order model did not match the actual results, demonstrating the poor interpretive ability of this model.

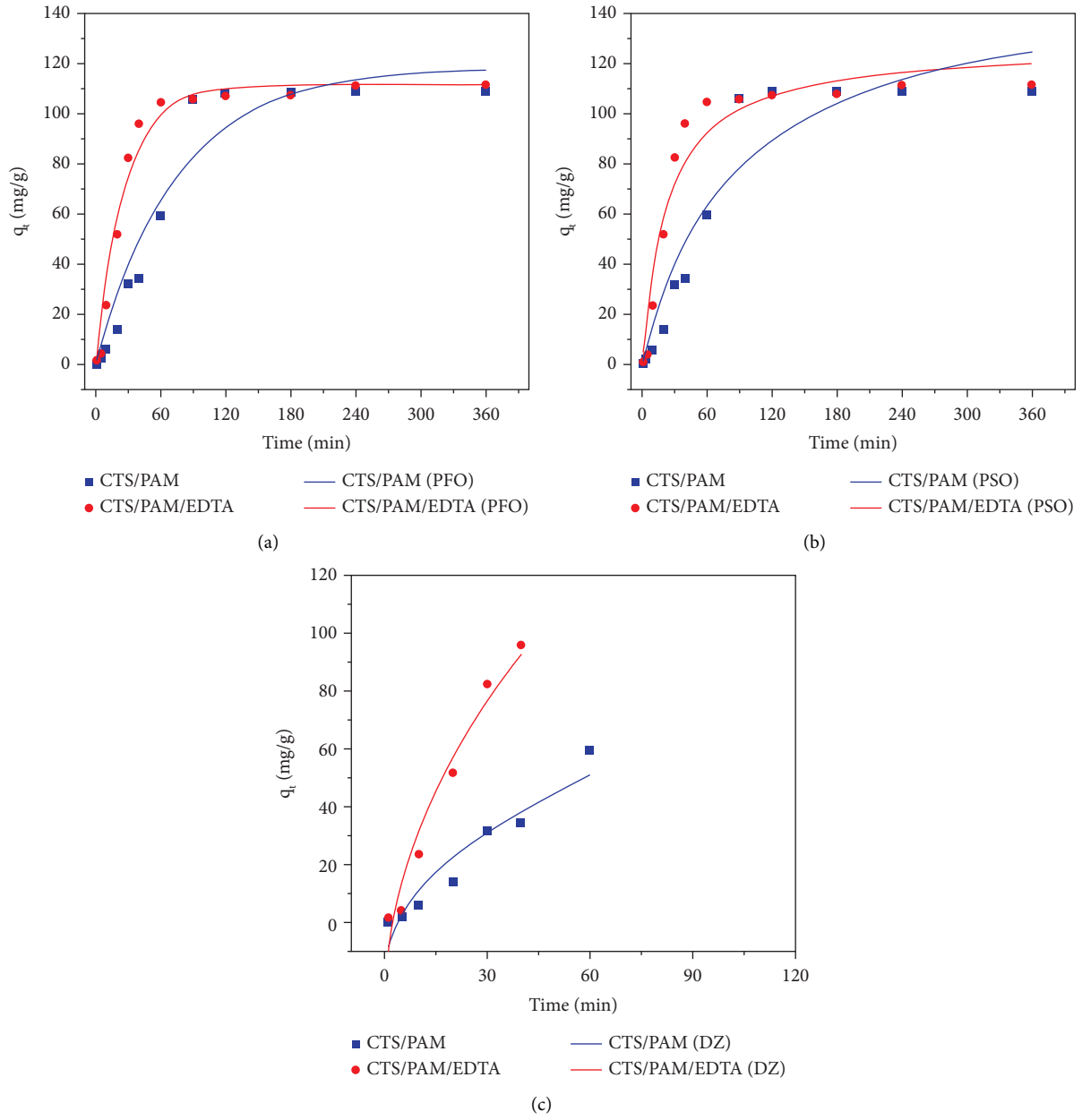

Figure 7: (a) Pseudo-first-order kinetic model, (b) pseudo-second order kinetic model, and (c) intraparticle kinetic model for CTS/PAM and CTS/PAM/EDTA hydrogels.

The intraparticle diffusion kinetic model for each adsorbent is shown in Figure 7(c). As can be observed, although the fit for CTS/PAM was $R^2 = 0.91$, the fit for CTS/PAM/EDTA was $R^2 = 0.95$, which was not a good fit compared to the pseudo-first-order model.

The obtained data represent that CTS/PAM and CTS/PAM/EDTA have significant efficiency for humic acid adsorption compared to CTS ($q_e = 111.66$ mg/g for CTS/PAM/EDTA, $q_e = 109.12$ for CTS/PAM, and $q = 29$ mg/g [25] for CTS at the same condition).

3.4. The Effect of Initial Concentration and Adsorption Isotherms. Adsorption isotherm models are useful in understanding the interactions between adsorbed molecules and active sites on the adsorbent surface [66]. Tables 2 and 3 show the data obtained from the adsorption of HA in different concentrations and at three temperatures of 25, 35, and 45°C at pH = 7. The results of the experiments show that with increasing temperature and initial concentration of HA, the adsorption capacity of both CTS/PAM and CTS/PAM/EDTA adsorbents had an upward trend. Therefore, HA adsorption is an endothermic adsorption process [67]. See Section 3 of the supporting information for further details.

Figures 8 and 9 demonstrate that adsorption capacity rises with increasing concentration and beginning temperature. At larger concentrations, HA offers a stronger driving force to overcome the barrier of mass transfer

Table 2: Amount of HA adsorbed at different concentrations and temperatures for CTS/PAM adsorbent.

Initial concentration (mg/L)	Adsorbed HA (mg/g)			Equilibrium concentration (mg/L)		
	25°C	35°C	45°C	25°C	35°C	45°C
40	71.20	71.65	72.10	4.39	4.17	3.94
50	90.61	91.05	91.80	4.69	4.47	4.09
60	109.11	109.57	110.31	5.44	5.21	4.84
70	128.22	128.67	129.11	5.88	5.66	5.44
80	146.58	147.47	148.52	6.70	6.26	5.73
90	164.53	166.43	167.17	7.23	6.78	6.41

Table 3: Amount of HA absorbed at different concentrations and temperatures for CTS/PAM/EDTA adsorbent.

Initial concentration (mg/L)	Adsorbed HA (mg/g)			Equilibrium concentration (mg/L)		
	25°C	35°C	45°C	25°C	35°C	45°C
40	74.79	75.08	75.68	2.60	2.45	2.15
50	93.44	94.64	95.08	3.27	2.67	2.45
60	111.66	113.29	114.49	4.17	3.35	2.75
70	130.31	132.10	133.29	4.84	3.94	3.35
80	148.22	150.46	151.50	5.88	4.76	4.24
90	166.58	168.22	169.41	6.70	5.88	5.25

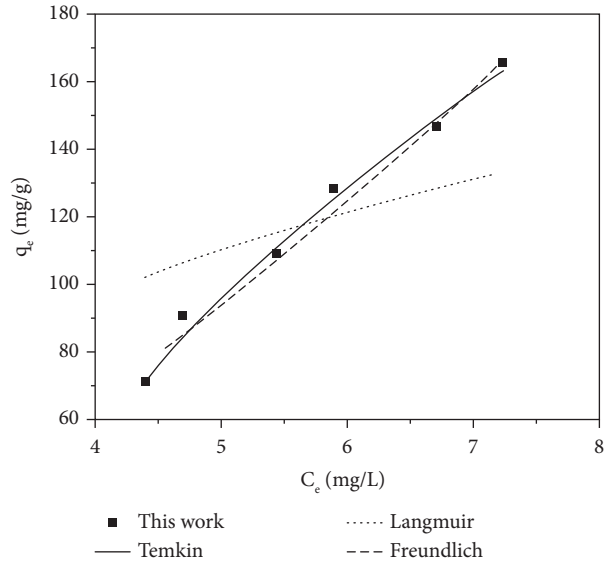

Figure 8: The effect of initial concentration on HA adsorption by CTS/PAM at 25°C for all three isotherm models.

between liquid and solid phases and also enhances the chance of collision between HA and hydrogel, resulting in an increase in adsorption capacity [68]. High temperature activates the active sites of the hydrogel and raises the hydrogel's kinetic speed, hence increasing the hydrogel's adsorption capacity [69]. This demonstrates that the HA adsorption pathway is endothermic [68]. In contrast, when the temperature rises, the HA bonds are likely to break, and the molecules will grow smaller, making it easier for the molecules to enter the adsorbent [21]. Three models of Langmuir, Freundlich, and Temkin isotherms were employed to study the adsorption process further and assess hydrogels' performance.

Tables 4 and 5 provide the isotherm parameters for each adsorbent. According to the results, the Temkin model with $R^2 = 0.991$ for CTS/PAM adsorbent and the Freundlich model with $R^2 = 0.997$ for CTS/EDTA adsorbent at 25°C have a good match and represent the process more accurately. Considering that Temkin's model provided the best match, the presence of heterogeneous surfaces on the adsorbent surface facilitated the adsorption of HA. As a result of the chemical adsorption of CTS/PAM/EDTA with HA, the cross-linking of EDTA is seen to boost the adsorption process. In addition, the connection between electron acceptor and donor, hydrophobic interactions, and hydrogen bonding all contributed to the adsorption of HA [61, 68].

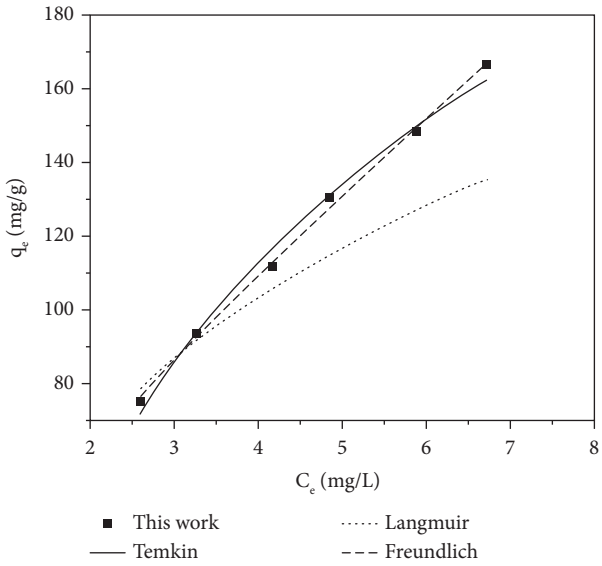

Figure 9: The effect of initial concentration on HA adsorption by CTS/PAM/EDTA at 25°C for all three isotherm models.

Table 4: Isotherm parameters for all three models for CTS/PAM adsorbent.

Isotherm	Parameters	Temperature		
		25°C	35°C	45°C
Langmuir	q_m (mg·g^{-1})	250	250	250
	K_L(l·mg^{-1})	0.157	0.135	0.146
	R_L^2	0.550	0.350	0.354
Freundlich	K_F ((mg·g^{-1}) (l·g^{-1})$^{1/n}$)	7.48	7.92	9.51
	n	0.641	0.627	0.644
	R_F^2	0.983	0.989	0.972
Temkin	b	1.13	1.56	2.049
	A	0.337	0.354	0.385
	R^2	0.991	0.990	0.974

Table 5: Isotherm parameters for all three models for CTS/PAM/EDTA adsorbent.

Isotherm	Parameters	Temperature		
		25°C	35°C	45°C
Langmuir	q_m (mg·g^{-1})	250	250	250
	K_L (l·mg^{-1})	0.175	0.209	0.244
	R_L^2	0.70	0.65	0.65
Freundlich	K_F ((mg·g^{-1}) (l·g^{-1})$^{1/n}$)	34.67	41.52	49.009
	n	1.212	1.237	1.304
	R_F^2	0.997	0.964	0.940
Temkin	b	2.17	2.826	3.67
	A	0.811	0.893	1.048
	R^2	0.990	0.988	0.975

3.5. The Influence of Ion Concentration on the HA Adsorption. In Figure 10, the influence of ion concentration, specifically NaCl, on the adsorption performance of HA is investigated. The impact of electrolytes on HA adsorption is crucial, as a variety of electrolytes with varying concentrations may either enhance or inhibit the adsorption process [70]. Additionally, HA's molecular structure is known to be influenced by ionic strength. High ionic strength potentially reduce charge repulsion between carboxylic or phenolic groups near HA, leading to a more complex structure.

To systematically examine the impact of ionic strength on HA adsorption, NaCl concentrations of 0.01 mol/L and 0.1 mol/L were compared to a HA solution without NaCl. Surprisingly, our findings in Figure 10 revealed a non-linear relationship between ion concentration and HA adsorption capacity. At 0.01 mol/L NaCl, there was a noticeable increase

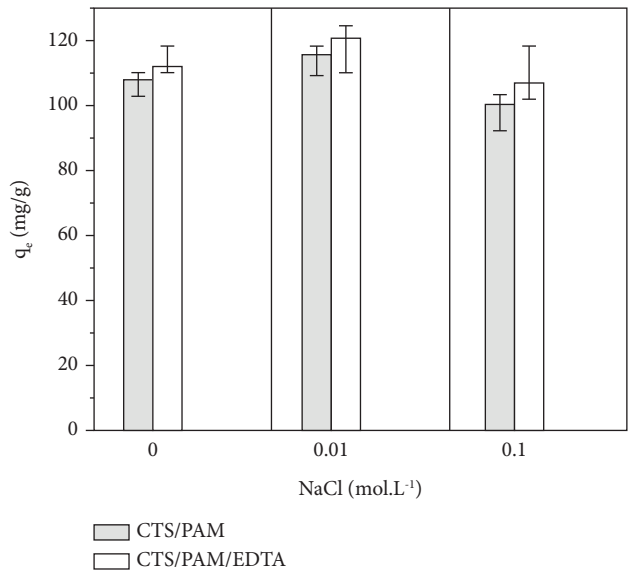

Figure 10: Effect of ion concentration on HA adsorption by CTS/PAM and CTS/PAM/EDTA.

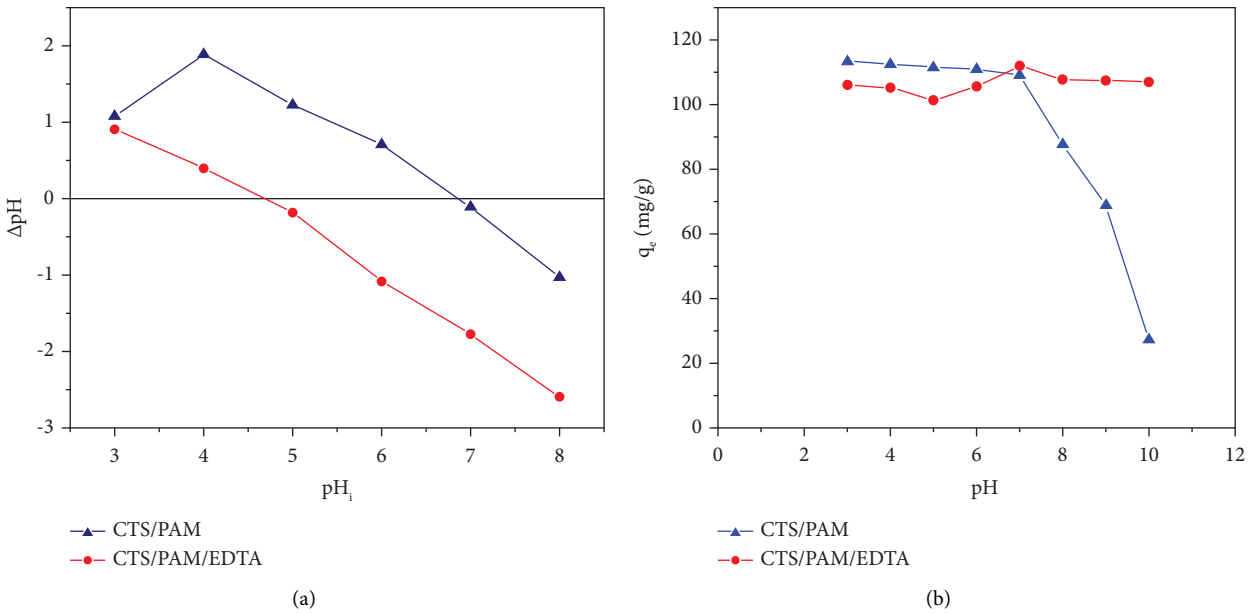

Figure 11: (a) point of zero charge (pH_{pzc}) of the adsorbents, (b) The effect of pH on the adsorption capacity by CTS/PAM and CTS/PAM/EDTA.

in adsorption capacity, indicating that the addition of ionic strength considerably enhanced the adsorption of HA. This initial increment may be attributed to the competitive interactions between chloride ions (Cl^-) and HA in the active regions of the hydrogel, leading to improved adsorption efficiency.

However, as the ion concentration further increased to 0.1 mol/L of NaCl, we observed a subsequent drop in adsorption capacity. This decline suggests that the competitive interactions between Cl^- and HA reach a point where they may start hindering the adsorption process, potentially leading to desorption or reduced affinity between HA and the hydrogel [68]. The intricate interplay of these factors contributes to the observed non-linear trend in Figure 10.

It is essential to note that the complexity of ion interactions with HA adsorption is highlighted by these contrasting observations at different ion concentrations. Therefore, the evaluation of the influence of ions on HA adsorption under the two investigated conditions, 0.01 mol/L and 0.1 mol/L NaCl, provides valuable insights into the intricate interplay between ionic strength and the adsorption capacity of the hydrogels in the water treatment process.

3.6. The Influence of pH on HA Adsorption. The solution's pH has a significant impact on HA's adsorption effectiveness. This has to do with the geometry of the HA molecule, the surface charge, and the functional group states on the adsorbent surface. In alkaline pHs, the phenolic and carboxylic groups of HA become negatively charged by losing a proton (H^+), causing the molecules to form an elongated shape due to the repulsive pull of these negatively charged groups. The functional groups are protonated by lowering the pH, and the repulsive effects are reduced, leading the molecule to acquire a complex and compact shape [71]. The effect of initial pH (3–10) on HA adsorption by CTS/PAM and CTS/PAM/EDTA hydrogel is shown in Figure 11. With increasing pH of the solution for CTS/PAM adsorbent, the quantity of adsorption decreases; the greatest amount of adsorption for CTS/PAM adsorbent was found at pH = 3, and the point of zero charge (pH_{pzc}) of the hydrogel was found at pH = 6.92. The hydrogel acquires a positive charge at $pH > pH_{pzc}$ owing to the formation of amino groups. Electrostatic adsorption between positively charged hydrogel and negatively charged HA molecules was principally responsible for the high adsorption capacity in the pH range (3–7); at the point where $pH < pH_{pzc}$, the surface of the hydrogel became negatively charged when the pH reached 10. Electrostatic interaction between the negatively charged hydrogel and HA molecules reduces adsorption capacity. Due to the presence of EDTA in the hydrogel structure, the pH_{pzc} of the CTS/PAM/EDTA adsorbent is around 4.7. The hydrogel has a positive surface charge at $pH < pH_{pzc}$. In contrast, producing electrostatic attraction by HA, which imparts a negative charge, enhances the adsorption capacity. The electrostatic interaction between the positively charged hydrogel and the negatively charged HA molecules is principally responsible for the high adsorption capacity in the pH range (3–4.5). However, as the pH climbed to 7, we observed an increase in adsorption, which may be a result of the protonation of HA in an acidic environment [71]. At a pH greater than pH_{pzc}, the hydrogel surface has a negative charge, and HA also has a negative charge. Electrostatic repulsion between negatively charged hydrogel and negatively charged HA molecules resulted in a decrease in HA adsorption capacity, although adsorption capacity increased, which may have been owing to pH variations throughout the adsorption process. This indicates that electrostatic interaction alone cannot account for the interactions between HA and adsorbents.

4. Conclusion

The results of the study state that the effectiveness of CTS/PAM and CTS/PAM/EDTA hydrogels, compared to pure chitosan, has been significantly changed in the adsorption process of humic acid from water, based on various investigations and analyses. Particularly, we have found that:

First, the time needed for the humic acid adsorption process has decreased by approximately 66% in the CTS/PAM/EDTA DN hydrogel compared to CTS/PAM, based on kinetics analysis. This indicates that the CTS/PAM/EDTA hydrogel is more efficient in adsorbing humic acid from water than CTS/PAM, as it requires less time for the adsorption process.

Second, the adsorption behavior of humic acid on the CTS/PAM/EDTA hydrogel is more mathematically consistent with the Freundlich isotherm throughout the adsorption process. The Freundlich isotherm suggests that the adsorbent (CTS/PAM/EDTA hydrogel) likely has multiple layers and physical adsorption, indicating that the adsorption process is more complex and involves a greater surface coverage of humic acid on the hydrogel.

On the other hand, the adsorption behavior of humic acid on CTS/PAM is more consistent with the Temkin isotherm, which suggests that the adsorption process on this adsorbent is more temperature-dependent. The Temkin isotherm indicates that the system's temperature may influence adsorption, and the adsorption capacity may change with temperature.

In a nutshell, the study indicates that the CTS/PAM/EDTA DN hydrogel is more effective in adsorbing humic acid from water compared to CTS/PAM, as it requires less time for adsorption to occur and exhibits different adsorption behavior, as indicated by the Freundlich and Temkin isotherms. These findings provide valuable insights into the performance and potential applications of the synthesized polymeric adsorbents for humic acid removal from water.

Data Availability

The data used to support the findings of this study are included in the article and the supplementary information file.

Disclosure

A preprint has previously been published [72].

Conflicts of Interest

The authors declare that they have no conflicts of interest or personal relationships that could have appeared to influence the work reported in this paper.

Authors' Contributions

Each author made significant contributions to the research and preparation of the article entitled "Investigating the adsorption of humic acid from water using CTS/PAM and CTS/PAM/EDTA adsorbents." Mahdi Alizadeh investigated the study, interpretated the data, and wrote the original draft. Sajjad Abdi conducted the experiments and collected and analyzed the data. S. Majid Abdoli provided supervision, administrated the project, and contributed to writing, reviewing, and editing. Hossein Hazrati provided supervision, project administration, and contributed to writing, reviewing, and editing. Mehdi Salami-Kalajahi and Mehdi Salami-Kalajahi served as advisors, contributed to project

administration, and provided review and editing. All authors have read and approved the final version of the manuscript and take responsibility for its content.

Supplementary Materials

The authors have submitted one supporting information file with this manuscript, comprising 3 sections, 2 figures, and 7 equations. This file includes comprehensive information about the important features of our research. The structures of the synthesized materials described in Section 1. The second section, titled "Adsorption Kinetics," extensively provides the theories of the adsorption kinetics that are used in this study. The comprehensive examination presented in this analysis enhances the understanding of adsorption kinetics that was investigated in this investigation. Furthermore, Section 3 of the supplementary data provides the mathematical details of the adsorption isotherms, which include the Langmuir, Freundlich, and Temkin models. Each of these models is distinguished by its unique assumptions and consequences, which are presented in the supporting information file of this study. (*Supplementary Materials*)

References

[1] J. A. Hawkes, C. Patriarca, P. J. Sjöberg, L. J. Tranvik, and J. Bergquist, "Extreme isomeric complexity of dissolved organic matter found across aquatic environments," *Limnology and Oceanography Letters*, vol. 3, pp. 21–30, 2018.

[2] N. Ajalli, M. Alizadeh, A. Hasanzadeh, A. Khataee, and J. Azamat, "A theoretical investigation into the effects of functionalized graphene nanosheets on dimethyl sulfoxide separation," *Chemosphere*, vol. 297, 2022.

[3] W. Mook and K. Rozanski, "Environmental isotopes in the hydrological cycle," *IAEA Publish*, vol. 39, 2000.

[4] W. K. Dodds, *Freshwater Ecology: Concepts and Environmental Applications*, Elsevier, London, UK, 2002.

[5] E. Menya, P. W. Olupot, H. Storz, M. Lubwama, and Y. Kiros, "Synthesis and evaluation of activated carbon from rice husks for removal of humic acid from water," *Biomass Conversion and Biorefinery*, vol. 12, no. 8, pp. 3229–3248, 2022.

[6] A. Sharma and R. Anthal, "Humic substances in aquatic ecosystems: a review," *International Journal of Innovative Research in Science, Engineering and Technology*, vol. 5, no. 10, 2016.

[7] M. Sillanpää, *Natural Organic Matter in Water: Characterization and Treatment Methods*, Butterworth-Heinemann, Oxford, UK, 2014.

[8] G. Kastl, A. Sathasivan, and I. Fisher, "A selection framework for NOM removal process for drinking water treatment," *Desalination and Water Treatment*, vol. 57, no. 17, pp. 7679–7689, 2016.

[9] S. M. Korotta-Gamage and A. Sathasivan, "A review: potential and challenges of biologically activated carbon to remove natural organic matter in drinking water purification process," *Chemosphere*, vol. 167, pp. 120–138, 2017.

[10] A. Salehpour, M. Alizadeh, N. Ajalli, and J. Azamat, "Arsenic removal from aqueous solution using PWN-type zeolite membrane: a theoretical investigation," *Journal of Molecular Liquids*, vol. 395, Article ID 123952, 2024.

[11] X. Zhu, J. Liu, L. Li et al., "Prospects for humic acids treatment and recovery in wastewater: a review," *Chemosphere*, vol. 312, Article ID 137193, 2023.

[12] W. Wang, W. Wang, Q. Fan, Y. Wang, Z. Qiao, and X. Wang, "Effects of UV radiation on humic acid coagulation characteristics in drinking water treatment processes," *Chemical Engineering Journal*, vol. 256, pp. 137–143, 2014.

[13] S. K. C. Saboon, S. Arshad, M. S. Amjad, and M. S. Akhtar, "Natural compounds extracted from medicinal plants and their applications, Natural Bio-active Compounds," *Production and Applications*, vol. 1, pp. 193–207, 2019.

[14] R. S. Hebbar, A. M. Isloor, B. Prabhu, A. M. Asiri, A. M. Asiri, and A. F. Ismail, "Removal of metal ions and humic acids through polyetherimide membrane with grafted bentonite clay," *Scientific Reports*, vol. 8, no. 1, p. 4665, 2018.

[15] J. Rook, A. Graveland, and L. Schultink, "Considerations on organic matter in drinking water treatment," *Water Research*, vol. 16, no. 1, pp. 113–122, 1982.

[16] M. Schnitzer and S. U. Kahn, "Humic substances in the environment," *Journal of Soils and Sediments*, vol. 18, 1972.

[17] W. H. Organization, *Guidelines for Drinking-Water Quality: Second Addendum*, World Health Organization, Geneva, Switzerland, 2008.

[18] S. Mohamadi, H. Hazrati, and J. Shayegan, "Influence of a new method of applying adsorbents on membrane fouling in MBR systems," *Water and Environment Journal*, vol. 34, no. S1, pp. 355–366, 2020.

[19] S. Beiki, E. Moniri, A. H. Hassani, and H. Ahmad Panahi, "Preparation and characterization of dendrimer-modified magnetite nanoparticles for adsorption of humic acid from aqueous solution," *ChemistrySelect*, vol. 5, no. 24, pp. 7197–7204, 2020.

[20] S. Wang, E. Li, Y. Li, J. Li, Z. Du, and F. Cheng, "Enhanced removal of dissolved humic acid from water using eco-friendly phenylalanine-modified-chitosan Fe3O4 magnetic nanoparticles," *ChemistrySelect*, vol. 5, no. 14, pp. 4285–4291, 2020.

[21] A. Daifullah, B. Girgis, and H. Gad, "A study of the factors affecting the removal of humic acid by activated carbon prepared from biomass material," *Colloids and Surfaces A: Physicochemical and Engineering Aspects*, vol. 235, no. 1-3, pp. 1–10, 2004.

[22] T. Karanfil, M. A. Schlautman, and W. J. Weber, "Impacts of dissolved oxygen on the sorption of humic substances and the subsequent inhibition of o-cresol ptake by granular activated carbon," *Water Research*, vol. 28, no. 7, pp. 1673–1678, 1994.

[23] M. Johns, E. Skogley, and W. Inskeep, "Characterization of carbonaceous adsorbents by soil fulvic and humic acid adsorption," *Soil Science Society of America Journal*, vol. 57, no. 6, pp. 1485–1490, 1993.

[24] C. Schulthess and C. Huang, "Humic and fulvic acid adsorption by silicon and aluminum oxide surfaces on clay minerals," *Soil Science Society of America Journal*, vol. 55, no. 1, pp. 34–42, 1991.

[25] W. S. W. Ngah and A. Musa, "Adsorption of humic acid onto chitin and chitosan," *Journal of Applied Polymer Science*, vol. 69, no. 12, pp. 2305–2310, 1998.

[26] T. Moriguchi, K. Yano, M. Tahara, and K. Yaguchi, "Metal-modified silica adsorbents for removal of humic substances in water," *Journal of Colloid and Interface Science*, vol. 283, no. 2, pp. 300–310, 2005.

[27] Q. Tao, Z. Xu, J. Wang, F. Liu, H. Wan, and S. Zheng, "Adsorption of humic acid to aminopropyl functionalized

SBA-15," *Microporous and Mesoporous Materials*, vol. 131, no. 1-3, pp. 177–185, 2010.

[28] A. Imyim and E. Prapalimrungsi, "Humic acids removal from water by aminopropyl functionalized rice husk ash," *Journal of Hazardous Materials*, vol. 184, no. 1-3, pp. 775–781, 2010.

[29] E. M. Ahmed, "Hydrogel: preparation, characterization, and applications: a review," *Journal of Advanced Research*, vol. 6, no. 2, pp. 105–121, 2015.

[30] Y. Lv, Z. Pan, C. Song, Y. Chen, and X. Qian, "Locust bean gum/gellan gum double-network hydrogels with superior self-healing and pH-driven shape-memory properties," *Soft Matter*, vol. 15, no. 30, pp. 6171–6179, 2019.

[31] M. Alizadeh, N. Ajalli, A. Hasanzadeh, and J. Azamat, "Chapter 20- Functionalized nanofibrous mats for gas separation applications," in *Functionalized Nanofibers*, K. Deshmukh, S. K. K. Pasha, A. Barhoum, and C. Mustansar Hussain, Eds., pp. 579–615, Elsevier, London, UK, 2023.

[32] X. H. Wang, F. Song, D. Qian et al., "Strong and tough fully physically crosslinked double network hydrogels with tunable mechanics and high self-healing performance," *Chemical Engineering Journal*, vol. 349, pp. 588–594, 2018.

[33] J. P. Gong, Y. Katsuyama, T. Kurokawa, and Y. Osada, "Double network hydrogels with extremely high mechanical strength," *Advanced Materials*, vol. 15, no. 14, pp. 1155–1158, 2003.

[34] Y. Yue, X. Wang, J. Han et al., "Effects of nanocellulose on sodium alginate/polyacrylamide hydrogel: mechanical properties and adsorption-desorption capacities," *Carbohydrate Polymers*, vol. 206, pp. 289–301, 2019.

[35] J. Yang, Y. Li, L. Zhu, G. Qin, and Q. Chen, "Double network hydrogels with controlled shape deformation: a mini review," *Journal of Polymer Science Part B: Polymer Physics*, vol. 56, no. 19, pp. 1351–1362, 2018.

[36] S. Bi, J. Pang, L. Huang, M. Sun, X. Cheng, and X. Chen, "The toughness chitosan-PVA double network hydrogel based on alkali solution system and hydrogen bonding for tissue engineering applications," *International Journal of Biological Macromolecules*, vol. 146, pp. 99–109, 2020.

[37] X. Xiang, G. Chen, K. Chen, X. Jiang, and L. Hou, "Facile preparation and characterization of super tough chitosan/poly (vinyl alcohol) hydrogel with low temperature resistance and anti-swelling property," *International Journal of Biological Macromolecules*, vol. 142, pp. 574–582, 2020.

[38] H. P. Cong, P. Wang, and S. H. Yu, "Stretchable and self-healing graphene oxide–polymer composite hydrogels: a dual-network design," *Chemistry of Materials*, vol. 25, no. 16, pp. 3357–3362, 2013.

[39] Q. Chen, L. Zhu, H. Chen et al., "A novel design strategy for fully physically linked double network hydrogels with tough, fatigue resistant, and self healing properties," *Advanced Functional Materials*, vol. 25, no. 10, pp. 1598–1607, 2015.

[40] M. A. Haque, T. Kurokawa, G. Kamita, and J. P. Gong, "Lamellar bilayers as reversible sacrificial bonds to toughen hydrogel: hysteresis, self-recovery, fatigue resistance, and crack blunting," *Macromolecules*, vol. 44, no. 22, pp. 8916–8924, 2011.

[41] X. Huang, S. Nakagawa, H. Houjou, and N. Yoshie, "Insights into the role of hydrogen bonds on the mechanical properties of polymer networks," *Macromolecules*, vol. 54, no. 9, pp. 4070–4080, 2021.

[42] T. Lin, M. Shi, F. Huang et al., "One-pot synthesis of a double-network hydrogel electrolyte with extraordinarily excellent mechanical properties for a highly compressible and bendable flexible supercapacitor," *ACS Applied Materials and Interfaces*, vol. 10, no. 35, pp. 29684–29693, 2018.

[43] Y. Wang, F. Chen, Z. Liu et al., "A highly elastic and reversibly stretchable all-polymer supercapacitor," *Angewandte Chemie*, vol. 131, no. 44, pp. 15854–15858, 2019.

[44] Y. H. Na, "Double network hydrogels with extremely high toughness and their applications," *Korea-Australia Rheology Journal*, vol. 25, no. 4, pp. 185–196, 2013.

[45] Y. Kong, Y. Zhuang, Z. Han et al., "Dye removal by eco-friendly physically cross-linked double network polymer hydrogel beads and their functionalized composites," *Journal of Environmental Sciences*, vol. 78, pp. 81–91, 2019.

[46] S. Tang, J. Yang, L. Lin et al., "Construction of physically crosslinked chitosan/sodium alginate/calcium ion double-network hydrogel and its application to heavy metal ions removal," *Chemical Engineering Journal*, vol. 393, Article ID 124728, 2020.

[47] J. Ma, T. Li, Y. Liu et al., "Rice husk derived double network hydrogel as efficient adsorbent for Pb (II), Cu (II) and Cd (II) removal in individual and multicomponent systems," *Bioresource Technology*, vol. 290, Article ID 121793, 2019.

[48] Y. Zhuang, F. Yu, J. Ma, and J. Chen, "Enhanced adsorption removal of antibiotics from aqueous solutions by modified alginate/graphene double network porous hydrogel," *Journal of Colloid and Interface Science*, vol. 507, pp. 250–259, 2017.

[49] F. Yu, T. Cui, C. Yang, X. Dai, and J. Ma, "κ-Carrageenan/Sodium alginate double-network hydrogel with enhanced mechanical properties, anti-swelling, and adsorption capacity," *Chemosphere*, vol. 237, Article ID 124417, 2019.

[50] F. He, Q. Zhou, L. Wang, G. Yu, J. Li, and Y. Feng, "Fabrication of a sustained release delivery system for pesticides using interpenetrating polyacrylamide/alginate/montmorillonite nanocomposite hydrogels," *Applied Clay Science*, vol. 183, Article ID 105347, 2019.

[51] M. Vakili, M. Rafatullah, B. Salamatinia et al., "Application of chitosan and its derivatives as adsorbents for dye removal from water and wastewater: a review," *Carbohydrate Polymers*, vol. 113, pp. 115–130, 2014.

[52] I. O. Saheed, W. D. Oh, and F. B. M. Suah, "Chitosan modifications for adsorption of pollutants–A review," *Journal of Hazardous Materials*, vol. 408, Article ID 124889, 2021.

[53] V. Van Tran, D. Park, and Y.-C. Lee, "Hydrogel applications for adsorption of contaminants in water and wastewater treatment," *Environmental Science and Pollution Research*, vol. 25, pp. 24569–24599, 2018.

[54] M. Tülü and K. E. Geckeler, "Synthesis and properties of hydrophilic polymers. Part 7. Preparation, characterization and metal complexation of carboxy functional polyesters based on poly (ethylene glycol)," *Polymer International*, vol. 48, no. 9, pp. 909–914, 1999.

[55] S. M. Abdoli, D. Bastani, and H. Bargozin, "Adsorption of phenol compounds by nanoporous silica aerogel," *Scientia Iranica*, vol. 22, pp. 992–1000, 2015.

[56] K. J. Buckler and P. J. Turner, "Oxygen sensitivity of mitochondrial function in rat arterial chemoreceptor cells," *The Journal of Physiology*, vol. 591, no. 14, pp. 3549–3563, 2013.

[57] F. C. Wu, P. H. Wu, R. L. Tseng, and R. S. Juang, "Use of refuse-derived fuel waste for the adsorption of 4-chlorophenol and dyes from aqueous solution: equilibrium and kinetics," *Journal of the Taiwan Institute of Chemical Engineers*, vol. 45, no. 5, pp. 2628–2639, 2014.

[58] H. Moussout, H. Ahlafi, M. Aazza, and H. Maghat, "Critical of linear and nonlinear equations of pseudo-first order and

pseudo-second order kinetic models," *Karbala International Journal of Modern Science*, vol. 4, no. 2, pp. 244–254, 2018.

[59] J. C. Morris and W. J. Weber, *Adsorption of Biochemically Resistant Materials from Solution: 2, Federal Water Pollution Control Administration, Basic and Applied Sciences Program*, 1966.

[60] Z. Zheng, L. Wu, Y. Han et al., "Gut microbiota-controlled tryptophan metabolism improves D-Gal/LPS-induced acute liver failure in C57BL/6 mice," *Engineering*, vol. 14, pp. 134–146, 2022.

[61] C. Dong, W. Chen, and C. Liu, "Preparation of novel magnetic chitosan nanoparticle and its application for removal of humic acid from aqueous solution," *Applied Surface Science*, vol. 292, pp. 1067–1076, 2014.

[62] S. K. Lagergren, "About the theory of so-called adsorption of soluble substances, Sven," *Vetenskapsakad. Handingarl*, vol. 24, no. 1898, pp. 1–39.

[63] Y. Ho and G. McKay, "A comparison of chemisorption kinetic models applied to pollutant removal on various sorbents," *Process Safety and Environmental Protection*, vol. 76, no. 4, pp. 332–340, 1998.

[64] J. Zhao, Z. Wang, S. Ghosh, and B. Xing, "Phenanthrene binding by humic acid–protein complexes as studied by passive dosing technique," *Environmental Pollution*, vol. 184, pp. 145–153, 2014.

[65] Y. F. Guan, C. Qian, W. Chen, B. C. Huang, Y. J. Wang, and H. Q. Yu, "Interaction between humic acid and protein in membrane fouling process: a spectroscopic insight," *Water Research*, vol. 145, pp. 146–152, 2018.

[66] M. A. Al-Ghouti and D. A. Da'ana, "Guidelines for the use and interpretation of adsorption isotherm models: a review," *Journal of Hazardous Materials*, vol. 393, Article ID 122383, 2020.

[67] S. Chowdhury, R. Mishra, P. Saha, and P. Kushwaha, "Adsorption thermodynamics, kinetics and isosteric heat of adsorption of malachite green onto chemically modified rice husk," *Desalination*, vol. 265, no. 1-3, pp. 159–168, 2011.

[68] D. Doulia, C. Leodopoulos, K. Gimouhopoulos, and F. Rigas, "Adsorption of humic acid on acid-activated Greek bentonite," *Journal of Colloid and Interface Science*, vol. 340, no. 2, pp. 131–141, 2009.

[69] Z. Liu and S. Zhou, "Removal of humic acid from aqueous solution using polyacrylamide/chitosan semi-IPN hydrogel," *Water Science and Technology*, vol. 2017, no. 1, pp. 16–26, 2018.

[70] J. J. Kipling, *Adsorption from Solutions of Non-electrolytes*, Academic Press, Cambridge, UK, 2013.

[71] B. A. G. de Melo, F. L. Motta, and M. H. A. Santana, "Humic acids: structural properties and multiple functionalities for novel technological developments," *Materials Science and Engineering: C*, vol. 62, pp. 967–974, 2016.

[72] M. Alizadeh, S. Abdi, S. M. Abdoli, H. Hazrati, and M. Salami-Kalajahi, "Investigating the adsorption of humic acid from water using CTS/PAM and CTS/PAM/EDTA adsorbents," *Research Square*, 2023.